

146x82mm (96 x 96 DPI)

1
2
3
4
5
6
7
8
9
10
11
12
13
14
15
16
17
18
19
20
21
22
23

Shuihong Pan,[†] Jun He,[‡] Chengjun Wang ^{†*} and Yuegang Zuo [§]

[†] College of Chemistry and Materials Engineering

Wenzhou University, Wenzhou 325035, China

[‡] Department of Chemical and Environmental Engineering

The University of Nottingham Ningbo China, Ningbo 315100, China

[§] Department of Chemistry and Biochemistry

University of Massachusetts Dartmouth, North Dartmouth, MA 02747, USA

*Corresponding author

Email: cjwang@wzu.edu.cn

Phone: (+86)15167765923, Fax: (+86) 577-86689300

ORCID: 0000-0001-8433-3512

Submitted to *Environmental Science & Technology Letters*

June 28, 2017

24 **ABSTRACT**

25 The photodegradation of dibutyl phthalate (DBP) over two-dimensional black phosphorene
26 (2D-BP) nanosheets, which were prepared by an environmental friendly solution exfoliation
27 process, in water was investigated under simulated-sunlight. When coexist with water, oxygen,
28 and light, 2D-BP nanosheets can generate the ROS species of $^1\text{O}_2$ and $\text{O}_2^{\cdot-}$ by energy transfer or
29 charge transfer from excited P^* to ground state of oxygen, respectively. The ROS species
30 generation is oxygen dependent and positive related with the amount of 2D-BP added. Results
31 from this study demonstrated that the photodegradation of DBP effectively accelerated via $^1\text{O}_2$
32 oxidation reaction and effects of $\text{O}_2^{\cdot-}$ were negligible due to its relative low oxidative reactivity.
33 The present study provides an excellent method for the removal of DBP phthalate from aqueous
34 solution, which might also be applicable to other photodegradable and water soluble organic
35 pollutants.

36

37

38

39

40

41

42

43

44

45

46

47 INTRODUCTION

48 Phthalate acid esters (PAEs), synthetic organic compounds mainly used as plasticizers for
49 many industrial production, are a class of ubiquitous water contaminants.¹⁻³ As PAEs are linked
50 together with polymeric materials by Van der Waals force and hydrogen bond rather than
51 chemical bond, they are easy to migrate into the environment during manufacture, use and
52 disposal.⁴⁻⁵ Owing to the significant hazards to the environment and the organism, some of the
53 PAEs are considered as ‘priority pollutants’ by the United states Environmental Protection
54 Agency,^{1,6} Dibutyl phthalate (DBP), as a potential endocrine disrupting compound, is one of the
55 most common short-chained phthalate esters, which has been frequently identified in natural
56 environmental water.⁷ Given that these pollutants are significantly toxic with potential
57 teratogenicity and carcinogenicity, an effective approach which can be applied to remove these
58 toxic contaminants from natural water is urgently needed.

59 Reactive oxygen species (ROS) could be produced by many photosensitizers under light
60 illumination, playing a key role in the degradation of organic contaminants.⁸⁻¹⁰ Generally
61 speaking, ROS refers to the substance which not only contains oxygen atoms but also possesses
62 active characteristics mainly including of singlet oxygen ($^1\text{O}_2$), hydroxyl radicals ($\cdot\text{OH}$), and
63 superoxide radicals (O_2^-). Owing to its strong oxidizing properties, ROS achieves the rapid
64 degradation of toxic organic compounds through deep oxidation.⁹ Among the ROS, the $\cdot\text{OH}$ is a
65 powerful oxidizing agent and could rapidly and non-selectively damage virtually all types of
66 organic contaminants.¹¹ Compared with $^1\text{O}_2$ and $\cdot\text{OH}$, O_2^- does not have strong oxidation ability
67 while it has important implications for degrading toxic pollutants. In the past few years, many
68 ROS generating materials have been explored such as various noble metals and metal-free
69 materials including graphene and silicon; however, to the best of our knowledge, apart from their

70 low water solubility and quantum yield, the above mentioned materials are greatly challenged
71 due to the lack of broad light absorption and poor biocompatibility.¹² Thus, it is highly desirable
72 to seek a new material preferably with high capability to produce ROS under the irradiation of
73 sunlight with long wavelength absorption and exceptional biocompatibility.

74 Black phosphorus (BP) has attracted scientific attention as a metal-free layered
75 semiconductor because of its unique optical properties and electric structure.¹³⁻¹⁶ Composed of
76 puckered layers of phosphorus by weak van der Waals interlayer interaction, BP can be
77 exfoliated from a bulk crystal into mono or few-layer BP nanosheets.¹⁷⁻¹⁸ Compared with other
78 two-dimensional (2D) materials, such as graphene and transition metal dichalcogenides
79 (TMDs), of which the former notoriously has a zero band gap while the latter exhibits an indirect
80 to direct band gap transition from bulk crystals to monolayer sheet, BP possesses a universally
81 tunable direct band gap from 0.3eV for the bulk to 2.0eV for the monolayer.¹⁹ In addition, few-
82 layer BP nanosheets has attractive electronic structure and properties, implying that they would
83 have high potential in photocatalytic application. The previous literature have reported that the
84 ultrathin BP nanosheets could be efficient metal-free semiconductor photosensitizers for the
85 generation of $^1\text{O}_2$ and have exceptional biocompatibility.^{12, 20} As a result of its broad working
86 spectrum, the few-layer BP nanosheets is considered a superior photosensitizer candidate in
87 accelerating photodegradation of pollutants.

88 Herein, in the present study, our aims were to prepare and characterize the mono and few-
89 layer 2D-BP nanosheets, to evaluate the performance and investigate the mechanism of the DBP
90 photodegradation over as-prepared 2D-BP nanosheets in water solution under simulated sunlight.
91 The photo-decomposition of organic pollutants with 2D-BP nanosheets investigated in this study
92 could become an attractive technique as promising candidate for water purification process.

93 MATERIALS AND METHODS

94 Except acetonitrile and methanol were chromatographic grade, all chemicals used in this
95 study were analytical grade and were used as received. De-ionized water was used throughout
96 the experiments. Chemical manufactures and reagents preparation are provided in **Text S1**. The
97 solution with dispersion of 2D phosphorene nanosheets were prepared by sonication assisted
98 liquid-phase exfoliation in ice water bath as presented in **Figure 1**. In details, 18 mL of deionized
99 water was added into a 100-mL beaker and covered with parafilm. And the water was bubbled
100 with high-purity nitrogen for 10 min to eliminate the dissolved oxygen to minimize/prevent the
101 oxidation of BP. Then 2.0 mg of the commercially available BP crystal powder was added to the
102 deionized water and immediately sealed followed by sonication (AS20500BT, Atuomatic
103 Science Instrument Co. Ltd., China) in ice water bath for 2 hours. The ice was mainly used to
104 keep the temperature of solution stable during sonication. The beaker was frequently shaken to
105 enhance the effectiveness of exfoliation and dispersion of BP crystal powders in water. Finally,
106 the prepared suspension containing homogeneous 2D phosphorene nanosheets was kept in
107 refrigerator until use. The morphology of BP before and after exfoliation was examined by
108 scanning electron microscope (FEI, Nova NanoSEM 200, USA). The structural characteristics of
109 pristine bulk BP and the BP nanosheets were investigated by Raman microspectrometer
110 (Renishaw, RM-1000, UK) at laser excitation wavelength of 532 nm. The UV-vis absorbance
111 spectrophotometry of the phosphorene nanosheets was investigated by UV spectrophotometer
112 (Shimadzu, UV-1800, Japan).

113 The DBP sample solutions for photolysis experiments were freshly prepared at
114 concentrations of 30 $\mu\text{g/mL}$ by diluting the DBP stock standard solutions in water. The effects of
115 BP nanosheets on DBP photodegradation were evaluated by spiking DBP standard solutions into

116 the BP nanosheets suspension containing different concentrations of BP before photolysis
117 experiments. A merry-go-round photochemical chamber reactor equipped with a 500 W Xenon
118 Lamp (290 - 800 nm; Bi-Lang instrument Co., Ltd, Shanghai, China) was used for all photolysis
119 experiments. All laboratory experiments were conducted under the same irradiation intensity.
120 Eight quartz photolysis tubes (40 mm i.d., containing 50 mL of solution) were held in the ring of
121 the merry-go-round accessory. The ring rotated within the reactor chamber at a speed 20 *rpm* to
122 give a uniform irradiation to the photolysis tubes. A hollow cylindrical lampshade with
123 circulated cooling water (the temperature was maintained at 25 °C) was employed to cool the
124 light bulbs. Tubes for the dark control samples were wrapped in aluminum foil. Aliquots of
125 samples (100 μL) were withdrawn at intervals of 1, 2, 4, 6 and 8 hrs and directly injected into
126 high performance liquid chromatography (HPLC) to analyze the concentration of DBP (The
127 HPLC analytical methods are provided in **Text S2**). All experiments were run in duplicate.

128 **RESULTS AND DISCUSSION**

129 **Characterization of prepared 2D-BP nanosheets.**

130 The morphologies of BP before and after exfoliation were examined by scanning electron
131 microscope (SEM). The layered structure of primitive bulk BP is clearly observed (**Figure 2a**).
132 The SEM image of the exfoliated BP nanosheets (**Figure 2b**) indicates that the structure of ultra-
133 thin mono and few-layer 2D-BP nanosheets was formed by the water exfoliation technology with
134 the assistant of sonication. The structural characteristics of pristine bulk BP and the as-prepared
135 ultra-thin 2D-BP nanosheets were investigated by Raman spectroscopy. As presented in **Figure**
136 **2c**, the Raman spectra of BP featured three characteristic peaks located at about 360, 437, and
137 465 cm^{-1} , which are marked as A_g^1 , B_{2g} , and A_g^2 modes of BP, respectively.^{23, 24} Interestingly,
138 the Raman spectra of BP before and after exfoliation showed nearly identical characteristic peaks,

139 illustrating the as-obtained 2D-BP nanosheets still maintained the crystal structure of pristine
140 samples. Compared with pristine bulk BP, the central frequency of A_g^2 modes in 2D-BP
141 nanosheets with obvious redshift is noted, while the shift of A_g^1 peak was not significant. In
142 addition, the intensity ratio A_g^1/A_g^2 in 2D-BP nanosheets increased greatly as compared to that in
143 bulk BP. According to previous work on exfoliated BP reported by Favron et al, it is known that
144 the central frequency of A_g^2 modes is most sensitive to changes in the number of layers and the
145 A_g^1 modes change is least significant as the thickness of layers is reduced.²¹ Consequently, A_g^2
146 modes with significant shift was observed. Hence, the successful preparation of mono and few-
147 layer 2D-BP nanosheets in this study could be confirmed by the Raman spectra.

148 The as-obtained 2D-BP nanosheets was further examined by UV-vis spectrophotometry
149 to determine their unique optical absorption properties. As presented in **Figure 2d**, the
150 UV-vis optical absorption spectra is consistent with the previous theoretical prediction
151 that the absorption of BP nanosheets is thickness dependent and their direct tunable band
152 gap covers a broad region ranging from 0.3 eV in the pristine bulk samples to 2.0 eV in the
153 single layer phosphorene.^{15, 19, 23} It is crucial for 2D-BP nanosheets to be effective
154 photosensitizers to possess an exceptional optical absorption properties.

155 **Accelerated photodegradation of DBP over 2D-BP nanosheets.**

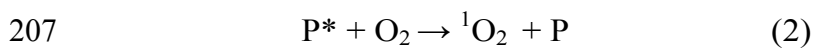
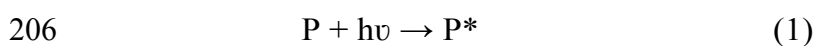
156 To evaluate the performance of 2D-BP nanosheets on photodegradation of DBP in
157 aqueous solution, the degradation efficiency of DBP containing suspended ultra-thin 2D-
158 BP nanosheets was carried out under the irradiation of xenon lamp. Specifically, the
159 purchased bulk BP (1mg or 2mg) was added to an anaerobic deionized water (19.4 mL)
160 that had been bubbled with nitrogen for 10 min to eliminate the dissolved oxygen, and
161 immediately sealed to prevent the solution from air. Afterwards, the mixture was

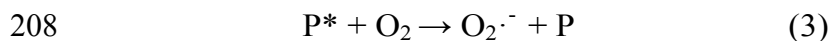
162 ultrasonicated in ice water for 2 hours and its color gradually changed from clear to the
163 dark brown as the BP was exfoliated (**Figure S1**). Then, 0.6 mL of DBP (0.1 mg/mL) was
164 added to the sample solution containing suspended ultra-thin 2D-BP nanosheets and
165 placed in the photo-reactor to conduct photodegradation tests. For comparison, the
166 aqueous DBP solution with bulk BP and without BP nanosheets was also tested under the
167 same conditions. As illustrated in **Figure 3a**, after 6 h irradiation, more than 45% of total
168 DBP was degraded in samples containing 2 mg of 2D-BP nanosheets while only 22%
169 DBP was decomposed without BP nanosheets. The photodegradation efficiency of DBP
170 gradually increased with the increase of BP quantity added (0, 1.0 and 2.0 mg), indicating
171 that the photodegradation of DBP was notably accelerated due to the presence of 2D-BP
172 nanosheets.

173 Given the exceptional absorption window from UV-Vis to near-infrared region and
174 unique electron accepting abilities, BP nanosheets could be excited under sunlight
175 irradiation and further generate ROS species which may be beneficial to the degradation
176 of organic compounds when water, oxygen and visible light are simultaneously present.²¹⁻
177 ^{22, 25} To evaluate the possible involvement of the ROS for the photodegradation of DBP
178 in the presence of BP nanosheets, the quenching experiments for reactive oxygen species
179 including $\cdot\text{OH}$, $^1\text{O}_2$ and $\text{O}_2\cdot^-$ were conducted (**Text S3**). As displayed in **Figure 3b**, the
180 degradation of DBP was significantly inhibited by adding DABCO, indicating that 2D-BP
181 nanosheets do generate the $^1\text{O}_2$, which is a dominant oxidizing agent and significantly
182 accelerates the photodegradation of DBP through deep oxidation. After adding a
183 quantitative amount of IPA and NBT as scavengers of $\cdot\text{OH}$ and $\text{O}_2\cdot^-$, the removal
184 efficiency of DBP showed negligible change (**Figure 3b**), further indicating the active

185 species generated by BP is singlet oxygen $^1\text{O}_2$ under light irradiation. However, the UV-
186 Vis absorption of NBT gradually decay with the light irradiation during the photolysis
187 process (**Figure S2**), implying the generation of $\text{O}_2\cdot^-$ consuming more NBT over time.
188 Therefore, the negligible contribution to the DBP degradation by $\text{O}_2\cdot^-$ due to its weak
189 oxidizing properties compared to $^1\text{O}_2$. Furthermore, to exclude the possible direct reaction
190 between DBP and photoexcited BP nanosheets, the photolysis of DBP was carried out
191 under continuous N_2 and O_2 purge, respectively. The removal efficiency of DBP decreased
192 under N_2 conditions, while dramatically increased under O_2 conditions. The oxygen
193 content dependent character clearly indicates that the $^1\text{O}_2$ is generated under
194 photosensitizing process by energy transfer from BP to ground-state oxygen. Although
195 both the ultrathin 2D-BP nanosheets and bulk BP can induce the formation of $^1\text{O}_2$, the
196 DBP decomposition efficiency in the case of ultrathin 2D-BP nanosheets is significantly
197 higher than that of corresponding bulk (**Figure 3a**). The dramatic enhancement of the $^1\text{O}_2$
198 generation would attribute to the ultrathin character of the nanosheets, which not only
199 provides rich surface atoms serving as the active sites but also reduces the electron-hole
200 recombination rate. Besides, the much higher charge-carried mobility of the ultrathin BP
201 nanosheets toward that of corresponding bulk sample would also benefit for the $^1\text{O}_2$
202 generation.

203 Overall, the generation of ROS species over 2D-BP nanosheets and accelerated
204 photodegradation mechanism of DBP when water, oxygen, 2D-BP nanosheets and light
205 coexist are proposed as follows:





210 Firstly, the electrons (e^-) on phosphorous are excited across the direct band gap to
211 the conduction band, creating excited P^* ; secondly, 1O_2 is generated through energy
212 transfer from P^* to ground state of O_2 or $O_2 \cdot^-$ is formed through a charge transfer reaction
213 under light; thirdly, DBP is decomposed via 1O_2 oxidation. Although the light induced
214 degradation of BP may affect its photocatalytic activity and need further modification for
215 industry applications, the high photocatalytic reactivity of 2D-BP nanosheets for organic
216 compounds decomposition could become an attractive technique for control of
217 environmental organic pollutants in water.

218 **ACKNOWLEDGMENTS**

219 The research project was jointly supported by the National Natural Science Foundation of
220 China (21477088) and Natural Science Foundation of Zhejiang Province (LY17B070001).

221 **NOTES**

222 The authors declare no competing financial interest.

223

224

225

226

227

228

229

230

231 **REFERENCES**

- 232 (1) Zheng, X. X.; Zhang, B. T.; Teng, Y. G. Distribution of phthalate acid esters in lakes of
233 Beijing and its relationship with anthropogenic activities. *Sci. Total Environ.* **2014**, 476-477,
234 107-113.
- 235 (2) Barreca, S.; Indelicato, R.; Orecchio, S.; Pace, A. Photodegradation of selected phthalates on
236 mural painting surfaces under UV light irradiation. *Microchem. J.* **2014**, 114, 192-196.
- 237 (3) Chen, Y. H.; Chen, L. L.; Shang, N. C. Photocatalytic degradation of dimethyl phthalate in an
238 aqueous solution with Pt-doped TiO₂-coated magnetic PMMA microspheres. *J. Hazard.*
239 *Mater.* **2009**, 172, 20-29.
- 240 (4) Peng, X. W.; Li, X. G.; Feng, L. J. Behavior of stable carbon isotope of phthalate acid esters
241 during photolysis under ultraviolet irradiation. *Chemosphere* **2013**, 92, 1557-1562.
- 242 (5) Mailhot, G.; Sarakha, M.; Lavedrine, B.; Cáceres, J.; Malato, S. Fe(III)-solar light induced
243 degradation of diethyl phthalate (DEP) in aqueous solutions. *Chemosphere* **2002**, 49, 525-
244 532.
- 245 (6) Yang, G. P.; Zhao, X. K.; Sun, X. J.; Lu, X. L. Oxidative degradation of diethyl phthalate by
246 photochemically-enhanced Fenton reaction. *J. Hazard. Mater.* **2005**, 126, 112-118.
- 247 (7) Lau, T. K.; Chu, W.; Graham, N. The degradation of endocrine disruptor di-n-butyl phthalate
248 by UV irradiation: A photolysis and product study. *Chemosphere* **2005**, 60, 1045-1053.
- 249 (8) Ciesla, P.; Kocot, P.; Mytych, P.; Stasicka, Z. Homogeneous photocatalysis by transition
250 metal complexes in the environment. *J. Mol. Catal. A: chem.* **2004**, 224, 17-33.
- 251 (9) Li, Y.; Zhang, W.; Niu, J. F.; Chen, Y. S. Mechanism of photogenerated reactive oxygen
252 species and correlation with the antibacterial properties of engineered metal-oxide
253 nanoparticles. *ACS Nano* **2012**, 6, 5164-5173.

- 254 (10) Lee, J.; Fortner, J. D.; Hughes J. B.; Kim, J. H. Photochemical Production of Reactive
255 Oxygen Species by C₆₀ in the Aqueous Phase during UV Irradiation. *Environ. Sci. Technol.*
256 **2007**, *41*, 2529-2535.
- 257 (11) Zhao, X. K.; Yang, G. P.; Wang, Y. J.; Gao, X. C. Photochemical degradation of dimethyl
258 phthalate by Fenton reagent. *J. Photoch. Photobio. A* **2004**, *161*, 215-220.
- 259 (12) Wang, H.; Yang, X. Z.; Shao, W.; Chen, S. C.; Xie, J. F.; Zhang, X. D.; Wang J.; Xie, Y.
260 Ultrathin Black Phosphorus Nanosheets for Efficient Singlet Oxygen Generation. *J. Am.*
261 *Chem. Soc.* **2015**, *137*, 11376-11382.
- 262 (13) Tran, V.; Yang, L. Scaling laws for the band gap and optical response of phosphorene
263 nanoribbons. *Phys. Rev. B* **2014**, *89*, 245407.
- 264 (14) Sun, Z. B.; Xie, H. H.; Tang, S. Y.; Yu, X. F.; Guo, Z. N.; Shao, J. D.; Zhang, H.; Huang,
265 H.; Wang, H. Y.; Chu, P. K. Ultrasmall Black Phosphorus Quantum Dots: Synthesis and Use
266 as Photothermal Agents. *Angew. Chem. Int. Ed.* **2015**, *54*, 11526-11530.
- 267 (15) Rahman, M. Z.; Kwong, C. W.; Davey, K.; Qiao, S. Z. 2D phosphorene as a water splitting
268 photocatalyst: fundamentals to applications. *Energy Environ. Sci.* **2016**, *9*, 709-728.
- 269 (16) Doganov, R. A.; O'Farrell, E. C.T.; Koenig, S. P.; Yeo, Y.; Ziletti, A.; Carvalho, A.;
270 Campbell, D. K.; Coker, D. F.; Watanabe, K. J.; Taniguchi, T. S.; Neto, A. H.; Ozyilmaz, C.
271 B. Transport properties of pristine few-layer black phosphorus by van der Waals passivation
272 in an inert atmosphere. *Nat. Commun.* **2015**, *6*, 6647.
- 273 (17) Bagheri, S.; Mansouri, N.; Aghaie, E. Phosphorene: A new competitor for graphene. *Int. J.*
274 *Hydrogen Energy* **2016**, *41*, 4085-4095.
- 275 (18) Lewis, E. A.; Brent, J. R.; Derby, B.; Haigh, S. J.; Lewis, D. J. Solution processing of two-
276 dimensional black phosphorus. *Chem. Commun.* **2017**, *53*, 1445-1458.

- 277 (19) Kang, J. H.; Wood, J. D.; Wells, S. A.; Lee, J. H.; Liu, X. L.; Chen, K. S.; Hersam, M. C.
278 Solvent Exfoliation of Electronic-Grade, Two-Dimensional Black Phosphorus. *ACS Nano*
279 **2015**, *9*, 3596-3604.
- 280 (20) Chen, W. S.; Yang, J. Q.; Liu, H.; Chen, M.; Zeng, K. J.; Sheng, P.; Liu, Z. J.; Han, Y. J.;
281 Wang, L. Q.; LI, J.; Deng, L.; Liu, Y. N.; Guo, S. J. Black Phosphorus Nanosheet-Based
282 Drug Delivery System for Synergistic Photodynamic/Photothermal/Chemotherapy of Cancer.
283 *Adv. Mater.* **2017**, *29*, 1603864.
- 284 (21) Favron, A.; Gaufres, E.; Fossard, F.; Phaneuf-L'Heureux, A-L.; Tang, N. Y-W.; Levesque,
285 P. L.; Loiseau, A.; Leonelli, R.; Francoeur S.; Martel, R. Photooxidation and quantum
286 confinement effects in exfoliated black phosphorus. *Nat. Mater.* **2015**, *14*, 826-832.
- 287 (22) Zhou, Q. H.; Chen, Q.; Tong, Y. L.; Wang, J. L. Light-Induced Ambient Degradation of
288 Few-Layer Black Phosphorus: Mechanism and Protection. *Angew. Chem. Int. Ed.* **2016**, *55*,
289 11437-11441.
- 290 (23) Guo, Z.; Zhang, H.; Lu, S. B.; Wang, Z. T.; Tang, S. Y.; Shao, J. D.; Sun, Z. B.; Xie, H. H.;
291 Wang, H. Y.; Yu, X. F.; Chu, P. K. From Black Phosphorus to Phosphorene: Basic Solvent
292 Exfoliation, Evolution of Raman Scattering, and Applications to Ultrafast Photonics. *Adv.*
293 *Funct. Mater.* **2015**, *25*, 6996-7002.
- 294 (24) Xu, J. Y.; Gao, L. F.; Hu, C. X.; Zhu, Z. Y.; Zhao, M.; Wang, Q.; Zhang, H. L. Preparation
295 of large size, few-layer black phosphorus nanosheets via phytic acid-assisted liquid
296 exfoliation. *Chem. Commun.* **2016**, *52*, 8107-8110.
- 297 (25) Ziletti, A.; Carvalho, A.; Campbell, D. K.; Coker, D. F.; Neto, A. H. C. Oxygen Defects in
298 Phosphorene. *Phys. Rev. Lett.* **2015**, *114*, 046801.
- 299
300

301

302 **Figure Captions**303 **Figure 1.** Schematic illustration of the fabrication process of water exfoliated 2D-BP nanosheets304 **Figure 2.** Scanning electron microscope (SEM) images of (a) the bulk BP before exfoliation and

305 (b) the exfoliated 2D-BP nanosheets; (c) Raman spectra and (d) UV-vis spectra of BP

306 nanosheets

307 **Figure 3.** Photodegradation of DBP in aqueous solutions (a) containing different types and

308 amounts of BP nanosheets; (b) containing 2 mg 2D-BP nanosheets and ROS quenchers

309

310

311

312

313

314

315

316

317

318

319
320
321
322
323
324
325
326
327
328
329
330
331
332
333
334
335
336
337
338
339
340
341
342
343

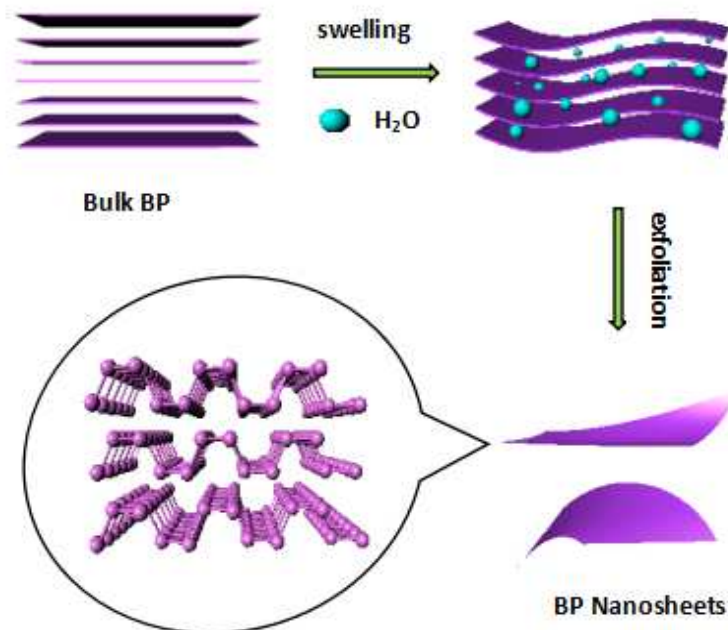
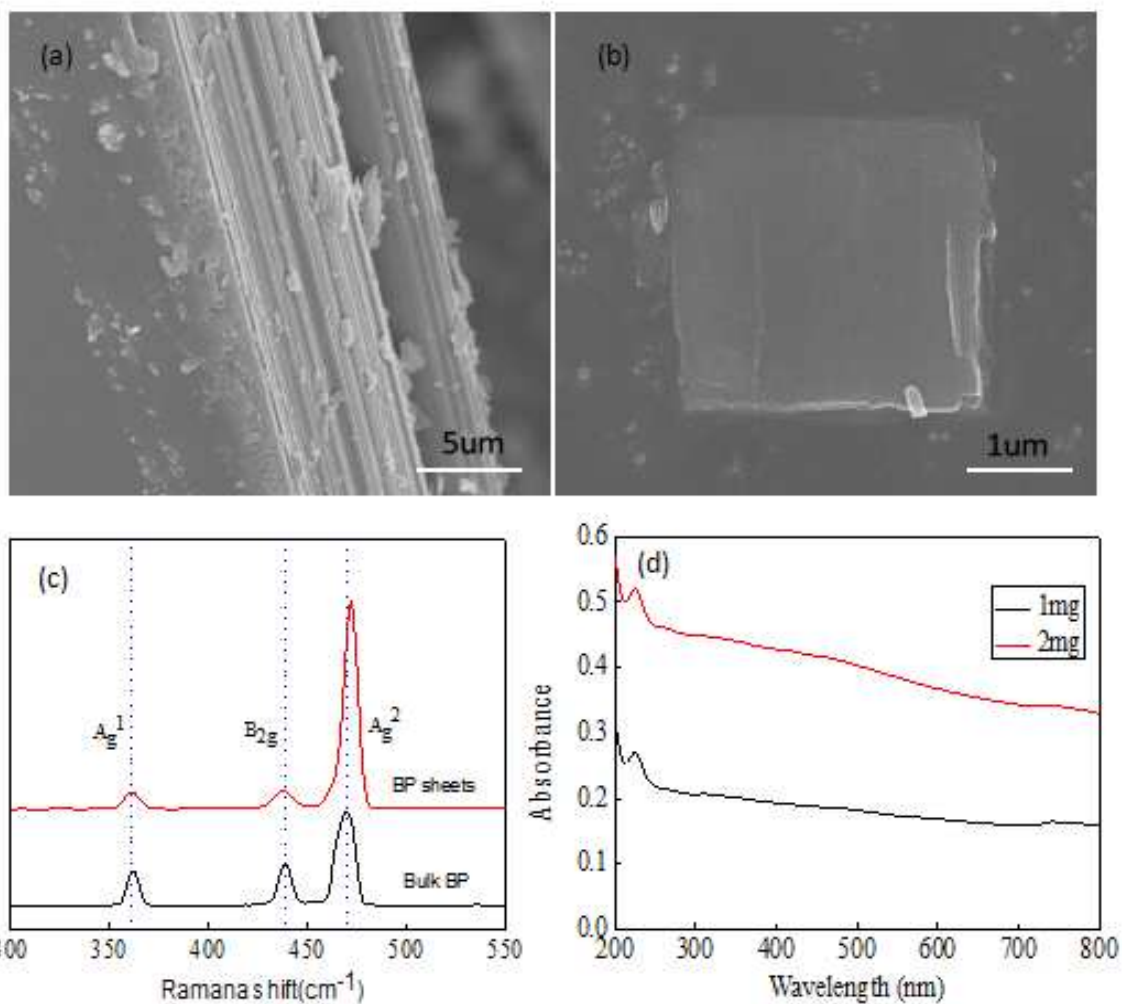


Figure 1. Schematic illustration of the fabrication process of water exfoliated 2D-BP nanosheets.

344

345

346



347

348 **Figure 2.** Scanning electron microscope (SEM) images of (a) the bulk BP before exfoliation and

349 (b) the exfoliated BP nanosheets; (c) Raman spectra and (d) UV-vis spectra of BP nanosheets

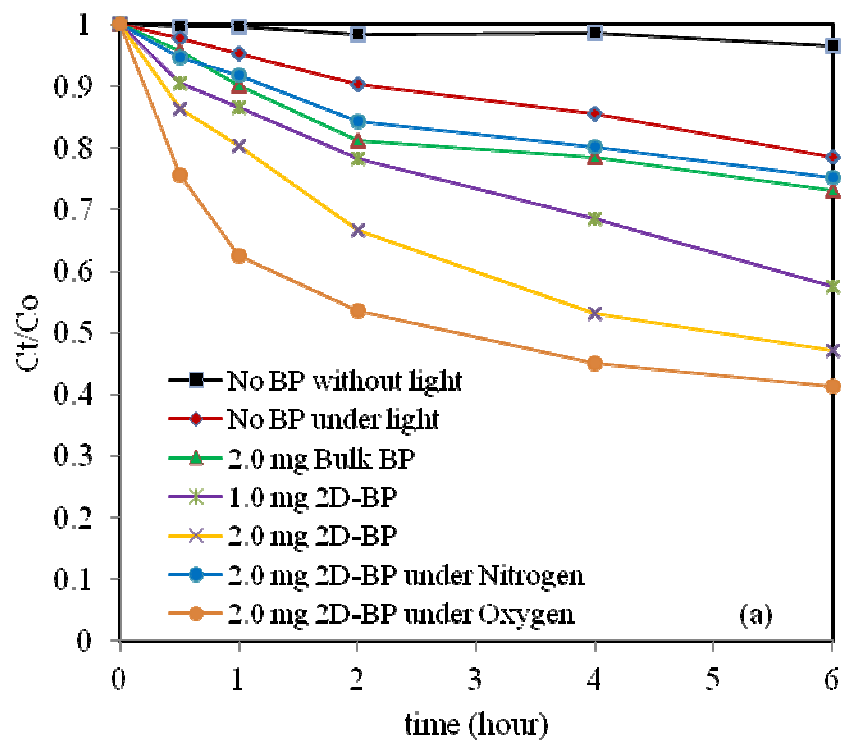
350

351

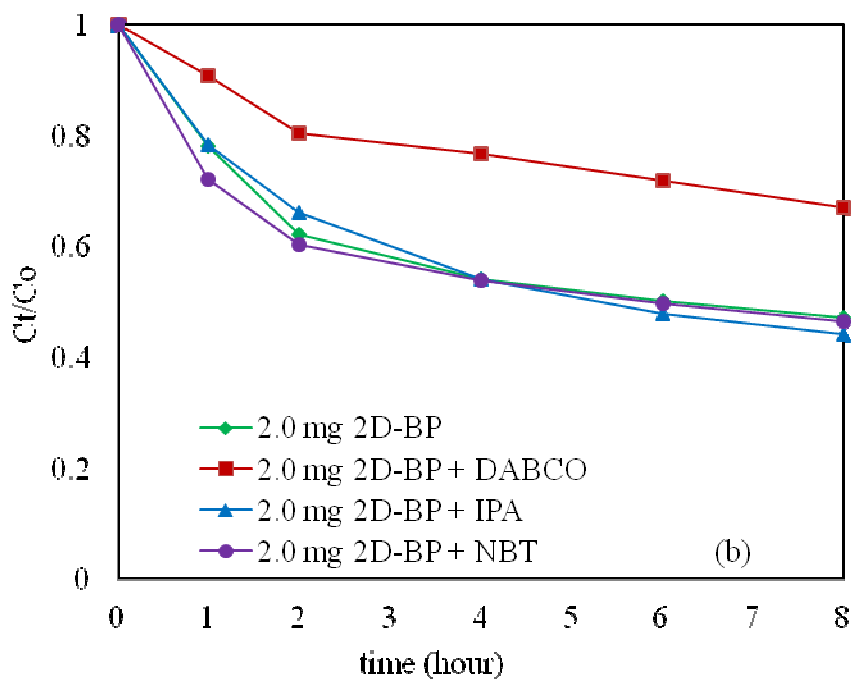
352

353

354



355



356

357 **Figure 3.** Photodegradation of DBP in aqueous solutions (a) containing different types and

358 amounts of BP nanosheets; (b) containing 2 mg 2D-BP nanosheets and ROS quenchers

359